World Journal of Applied Physics
2017; 2(4): 113-118
http://www.sciencepublishinggroup.com/j/wjap
doi: 10.11648/j.wjap.20170204.14

Theoretical Studies of Positron Annihilation in Aluminum Bismuth Alloy

Noureddine Amrane, Maamar Benkraouda

Faculty of Science, United Arab Emirates University, Al-Ain, United Arab Emirates

Email address:
namrane@uaeu.ac.ae (N. Amrane), maamar@uaeu.ac.ae (M. Benkraouda)

To cite this article:
Noureddine Amrane, Maamar Benkraouda. Theoretical Studies of Positron Annihilation in Aluminum Bismuth Alloy. *World Journal of Applied Physics*. Vol. 2, No. 4, 2017, pp. 113-118. doi: 10.11648/j.wjap.20170204.14

Received: July 30, 2017; **Accepted**: September 5, 2017; **Published**: November 11, 2017

Abstract: Electron and positron charge densities are calculated as a function of position in the unit cell for Aluminum Bismuth binary compound. Wave functions are derived from pseudopotential band structure calculations and the independent particle approximation (IPM), respectively, for the electrons and the positrons. It is observed that the positron density is maximum in the open interstices and is excluded not only, from the ion cores but also to a considerable degree from the valence bonds. Electron-positron momentum densities are calculated for (001, 110) planes. The results are used to analyze the positron effects in AlBi.

Keywords: Positron, Band Structure, Charge Density, Momentum Density

1. Introduction

The surfaces of III-V semiconductor compounds are of vital importance because the functioning of modern electronic devices is strongly influenced by their cleanliness, geometries, and photoelectric properties [1, 2]. Compared to other III-V materials, less is known about bismuth GaBi, AlBi and InBi binaries. While Bi is the last element in the Group-V column in the Periodic Table, it has been largely neglected as a member of the III-V compound semiconductor family which plays a significant role in modern electronic and optoelectronic device applications nowadays. This is, to large extent, due to the difficulties in synthesizing high quality binary III-Bi crystals and alloying Bi into host III-Vs. the first interest to incorporate Bi into III-Vs was stimulated by the isoelectronic trap discovered in O-doped ZnTe in 1962 [3] and later in N-doped GaP in 1965 [4]. When the substituted Group-V element has a large difference in electronegativity (3.04, 2.19, 2.18, 2.05 and 2.02 in Pauling scale for N, P, As, Sb and Bi, respectively) with respect to the host Group-V element, isoelectronic traps can be formed.

Positron annihilation experiments [5] have been used to investigate the electronic structure of pure metals, alloys and metals containing defects such as mono-vacancies, dislocations and large voids resulting from neutron irradiation. If the results of the experiments are to be used to obtain information about the electronic structure in these systems, it is important to have some knowledge of the spatial distribution of the annihilating positron.

Experiments and theory indicate that the measured two-photons angular correlation curves reflect the momentum space density of the electrons seen by injected positrons and contain information about the occupied regions of k-space [6], i.e. the Fermi surface [7]. The investigation of the electronic properties of solid by use of electronic and positronic charge densities represents an area of increasing importance. So far, most of the work has concerned electron charge densities as this has been found useful for the understanding of chemical bonds and recently for the modification of band structures by interstitial impurities [8, 9]. The great success of recent developments in this field provokes us to ask for a better understanding of the charge densities. We will show that both electronic and positronic charge densities could provide complementary information about the structure of semiconductors.

On the theoretical side, there has been some attempt to study the behavior of the positron wave function in compound semiconductors and alloys. This paper reports a theoretical framework for calculating the distribution of thermalized positrons and the electron pseudo-charge density for AlBi compound. The theoretical calculations of the line shapes are carried out employing the pseudopotential band model for the computation of the electron wave function. The positron wave function is evaluated under the point core

approximation (the independent particle model). The crystal potential experienced by a positron differs from that experienced by an electron. Since we assume that there is at most one positron in the crystal at any time, there are no positron-positron interactions, i-e. exchange or corrections. Thus positron potential results from a part due to the nuclei and another part due to the electrons, both components being purely Coulombic in nature.

The density functional theory (DFT) combined with the local density approximation (LDA) or with the generalized gradient approximation (GGA) [10, 11, 12] is one of the most efficient methods for electron-structure calculations, it has also been used for positrons states in bulk metals in order to determine the momentum distribution of the annihilating positron-electron pairs [13]. However, those calculations are technically difficult and computationally time consuming. It is well known that electronic structure based on the DFT calculations underestimates the band gaps by as much as 50-100%. The LDA, also overestimates the positron annihilation rate in the low-momentum regime, thus giving rise to shorter positron lifetimes than the experimental values. Moreover, the LDA overestimates the cohesive energy in electronic structure calculations, for reasons connected with the shape of the correlation hole close to the nucleus. The empirical methods [14, 15, 16], while simple in nature, and with the drawback that a large number of fitting parameters are required, are very accurate and produce electronic and positronic wave functions that are in good agreement with experiments. This approach was encouraged by the work of Jarlborg et al who discovered that the empirical pseudopotentials gave a better agreement with the experimental electronic structures than the first-principles calculations [17].

Computational details are given in section 2, and section 3 is devoted to the discussion of the results.

2. Method

The calculations are performed within the framework of the empirical pseudo-potential method, that has shown to give excellent results to experiments for bulk materials, and the coupling of this method to the independent particle model (IPM) is able to predict interesting properties of the positron's behavior in semiconductors.

The electron and positron wave functions are essential ingredients in the calculation of the electron-positron k-space densities. We therefore focus our attention to the evaluation of electron wave function derived from band structure calculation. One of the central problems in the band theory of solids is to find the propagating solution of a Schrodinger equation in which the potential has the periodicity of the lattice. Exact solutions of this problem are in general not possible, and so a number of approximation methods have been used in the past.

$$\left\{\frac{p^2}{2m}+V(r)\right\}\psi_{nk}(r)=E_{nk}\psi_{nk}(r) \tag{1}$$

In our case, we have used the empirical pseudo-potential method (EPM) [18], which involves a direct fit of the atomic form factors V(G) to the experimental band structure. Therefore, the first step in this calculation is to choose the best possible set of form factors, which will probably describe the band structure. The experimentally known energy gaps at Γ, X and L points of the Brillouin zone are taken as criteria.

$$H=-\frac{\hbar^2}{2m}\nabla^2+V(r) \tag{2}$$

The pseudo-potential Hamiltonian contains an effective potential which is expended as Fourier series in reciprocal lattice space. For a binary compound, the expansion is written in two parts which are symmetric and antisymmetric with respect to an interchange of two atoms about their midpoint.

$$V(r)=\sum_G\left[S^S(G)V^S(G)+iS^A(G)V^A(G)\right]\exp(iG.r) \tag{3}$$

The structure and form factors are as follows:

$$S^S(G)=\cos(G.\tau),\qquad S^A(G)=\sin(G.\tau) \tag{4}$$

$$V^S(G)=\frac{1}{2}(V^c(G)+V^A(G)) \tag{5}$$

$$V^a(G)=\frac{1}{2}(V^c(G)-V^A(G)) \tag{6}$$

Here, τ=(a/8) (111) is half the vector between two atoms contained in the unit cell and $V^c(G)$ and $V^A(G)$ are the pseudo-potential from factors of the individual atoms (we shall refer, hereafter, to the two sites A and C in the unit cell as anion and cation sites, respectively).

The pseudo wave functions $\psi_{nk}(r)$ have the Bloch form and they can be expanded in a set of plane waves, then we have:

$$\psi_{nk}(r)=\frac{1}{\sqrt{\Omega}}\sum C_{nk}(G)\exp(iGr) \tag{7}$$

The coefficients $C_{nk}(G)$ are found out by solving the secular equation.

The valence electron density $\rho(\mathrm{r})$ is defined as

$$\rho(r)=2\sum_n\sum_k\left|\psi_{nk}(r)\right|^2 \tag{8}$$

Where ψ_{nk} is the wave function of the valence electron with the wave vector k in the n-th valence band. The summations are taken over the occupied states (we have used about 1200 k-points). The charge density is eρ(r), where e is the electron charge.

This has the Fourier transform given by

$$\rho(G)=\frac{1}{\Omega}\int\rho(r)\exp(iG.r)d^3r \tag{9}$$

We follow the approach presented in. [19] for evaluating the positron wave function. With the assumption that there is only one positron for many electrons, there is no exchange part because there is no positron-positron interaction. The total positron potential can be expressed as

$$V_p(r) = V_i(r) + V_c(r) + V_{ep}(r) \tag{10}$$

where $V_i(r)$, $V_c(r)$, and $V_{ep}(r)$ are the ionic, Coulomb, and electron-positron correlation potentials, respectively. As explained in section I the electron-positron potential is not considered here.

In the point core approximation

$$v_i(r) = Ze^2/r \tag{11}$$

Since the positron moves in the Coulomb field of the nuclei and the electron, the corresponding potential may be written in atomic units as

$$v_c(r) = -2\int \frac{\rho(r')d^3r}{|r-r'|} \tag{12}$$

The wave function of the thermalized positron is given by:

$$\psi_+(r) = \frac{1}{\sqrt{\Omega}} \sum A(G)\exp(iGr) \tag{13}$$

The coefficients A(**G**) are found out by solving the secular equation for the positron. The positron can be described by a band model with one positron per unit cell independent-particle model (IPM) (20, 21). A fully thermalized positron is assumed to be, in good approximation, at the bottom of the positron band with k=0 and n=1.

The probability of annihilation of the $e^- - e^+$ pair with momentum p is proportional to the pair momentum density:

$$\rho^{2\gamma}(p) = \sum_{n,k} \eta_n(k) \left| \int d^3r \exp(-ip.r)\psi_{n,k}(r).\psi_+(r) \right|^2 \tag{14}$$

where $\psi_{n,k}(r)$ and $\psi_+(r)$ are the electron and positron Block wave functions and $\eta_n(k)$ is the occupation number. In the long-slit angular correlation experiment one measures a component of the pair momentum density as given by

$$N(p_z) = \iint \rho^{2\gamma}(p)dp_x dp_y \tag{15}$$

The parameters used for this calculation are listed in table 1, the calculated Fourier coefficients of the valence charge densities for AlBi are given in table 2.

3. Results

In the first step of our calculations, we have computed the Fourier coefficients of the valence charge densities using the empirical pseudopotential method (EPM). This method has been proved to be largely sufficient to describe qualitatively the realistic charge densities. As input, we have introduced the form factors (the symmetric and antisymmetric parts) and the lattice constant for AlBi. The resulting Fourier coefficients are used to generate the corresponding positron wave function using the IPM.

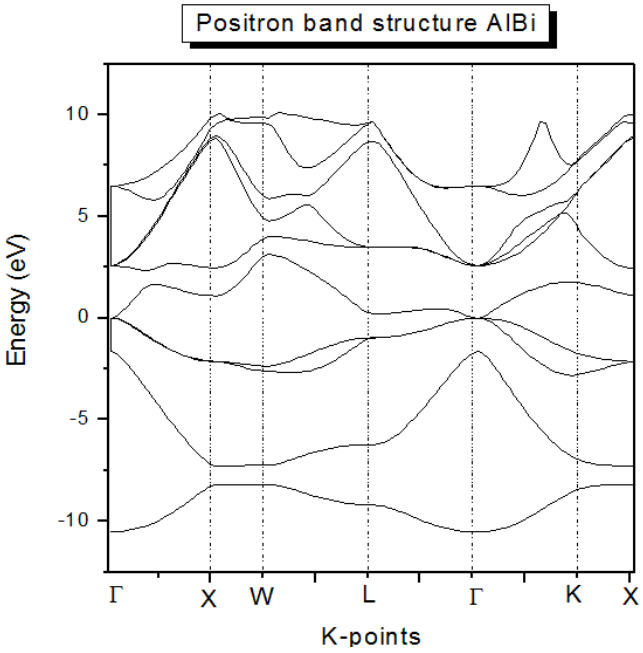

Figure 1. *Positron band structure versus K-points.*

The positron band structure for Albi is displayed in figure 1, we note the astonishing similarity with its electron counterpart, with the exception that the positron energy spectrum does not exhibit a band gap. This is consistent with the fact that these bands are all conduction bands. The calculated positron charge densities in the (110) plane and along the <111> direction are displayed in Figures (2a, 2b), it is seen that the positron is located in the interstitial region and that the probability is low around the positions of the nuclei. The positron is repelled by the positively charged atomic cores and tends to move in the interstitial regions. The maximum of the charge is located at the tetrahedral site. From a quantitative point of view, there is a difference of charge in the interstitial regions, the positron distribution is more pronounced in the neighborhood of the Bi cation than in that of the Al anion. These differences in profiles are immediately attributable to the cell which contains the larger valence and the larger ion core. We are considering the implications of this in regard to the propensity for positron trapping and the anisotropies that might be expected in the momentum densities for both free and trapped positron states. We should point out that the good agreement of the band structure and charge densities were used as an indication of both the convergence of our computational procedure and the correctness of the pseudopotential approach using the adjusted form factors, these latter as well as the lattice constant have been adjusted to the experimental data before the calculations.

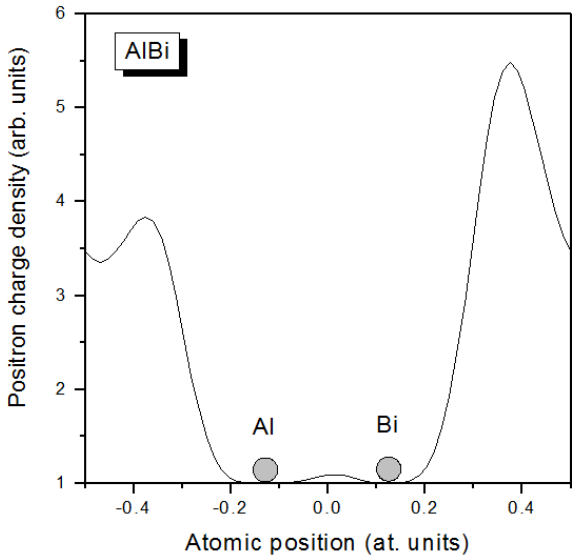

Figure 2a. *Positron charge density versus Atomic position.*

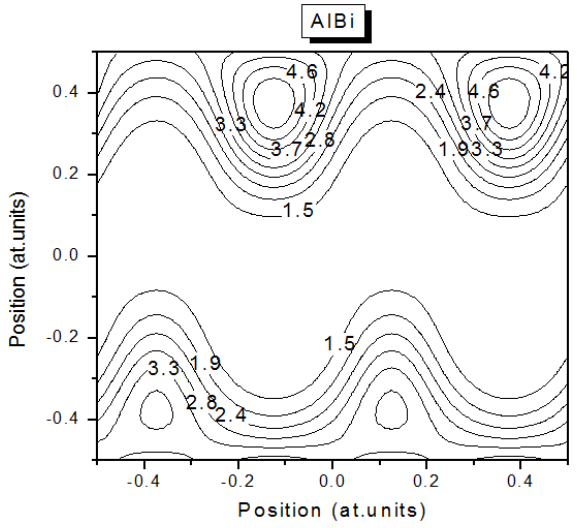

Figure 2b. *Position versus position.*

Let us now discuss the results of the calculated 2D-electron-positron momentum density for AlBi, obtained by integration of the appropriate plane along the <110> and <001> directions (Figures 3 and 4), the first obvious observation is that the profiles exhibit marked departures from simple inverted parabola, suggesting that for AlBi the electrons behave as nearly free (NFE). At the low momentum region, the profile along the <001> direction is seen to be flat as observed in Ge and Si [22]. Compared to this, the profile along the <110> direction is sharply peaked. However, the valleys and dips observed in $\rho(p)$ for AlBi are very shallow as compared with those of Si and Ge. This fact clearly tells us that the momentum dependence of $\rho(p)$ is very much different between elemental and compound semiconductors. In the case of Si, the symmetry is O_h^7 which contains 48 symmetry operations including glide and screw, in the case of AlBi, the symmetry is lowered from O_h^7 to T_d^2 : the two atoms in each unit cell are inequivalent and the number of symmetry operations thus decreases from 48 to 24. Since the glide and the screw operations are not included in this space group, this crystal is symmorphic. It is emphasized that the symmetry lowering from O_h to T_d revives some of the bands which are annihilation inactive in the case of Si. If this symmetry lowering effect is large enough, the ratio in the annihilation rate of the [110] line to the [001] one becomes small since the bands become annihilation active for both ridge [110] and valley [001] lines. From the calculations performed by Saito et al. [23] in GaAs, it was found that the contribution of these revived bands to the annihilation rate is small. The sharp peaking along the <110> direction and the flatness of the peak along the <001> direction could also be understood in terms of the contribution of σ and π^* orbitals to the ideal sp^3 hybrid ones. Since the electronic configuration of Aluminum is $1s^2 2s^2 2p^6 3s^2 3p^1$ and that of Bismuth is [Xe] $4f^{14}5d^{10}6s^2 6p^3$, the interaction between second neighbor σ bonds is equivalent to a π antibonding interaction between neighboring atoms. As a consequence, there is a strong (2p, 2p) σ bond along <110> direction and an admixture of (2p, 2p) σ and (2p, 2p) π^* bonds along <001> direction, the explanations are in good agreement with an earlier analysis based on group theory [8].

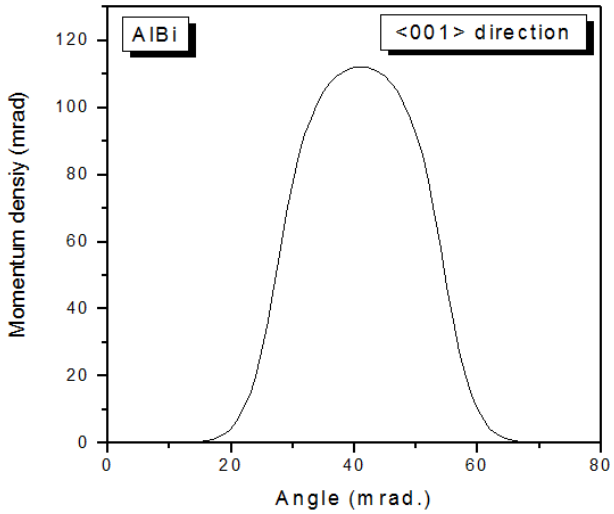

Figure 3. *Momentum density versus angle (001).*

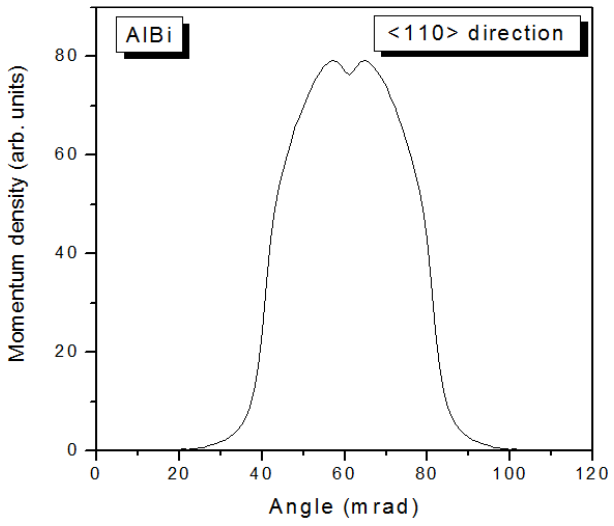

Figure 4. *Momentum density versus angle (110).*

The calculated electron-positron momentum density (contour maps and bird's eye view of reconstructed 3D momentum space density) in the (110-001) plane is displayed in Figure 5 and 6. There is a good agreement in the qualitative feature between our results and experimental data obtained by Berko and co-workers for carbon [24], one can notice that there is a continuous contribution, i.e. there is no break, thus all the bands are full. The contribution to the electron-positron momentum density are at various $p = k+G$. In case of elemental semiconductors like Si, a set of bonding electrons is composed of 3p electrons, the distortion is expected to be observed since both of the 2p and 3p set of electrons possess a perfect point symmetry. But it can be seen that for AlBi, the degree of distortion is smaller than in Si. Compared to this result, the number of contour lines is smaller and the space between the contour lines is wider in AlBi system.

Figure 7 gives the calculated LCW folded distribution for AlBi. The momentum distribution in the extended zone scheme is represented by n(k) in the reduced zone scheme. We can deduce from the map that the electronic structure consists entirely of full valence bands, since the amplitude variation in the LCW folded data is merely constant.

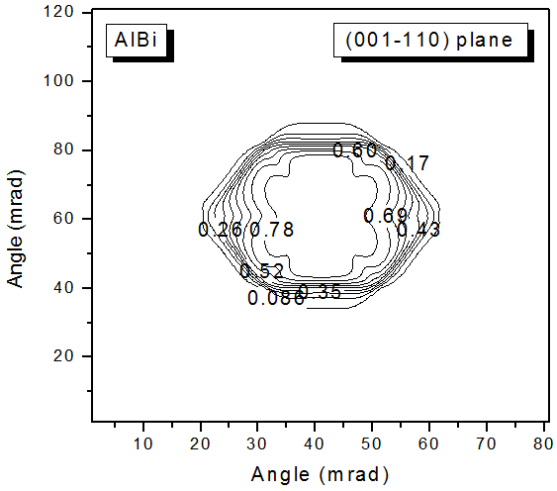

Figure 5. *Angle versus angle (001-110).*

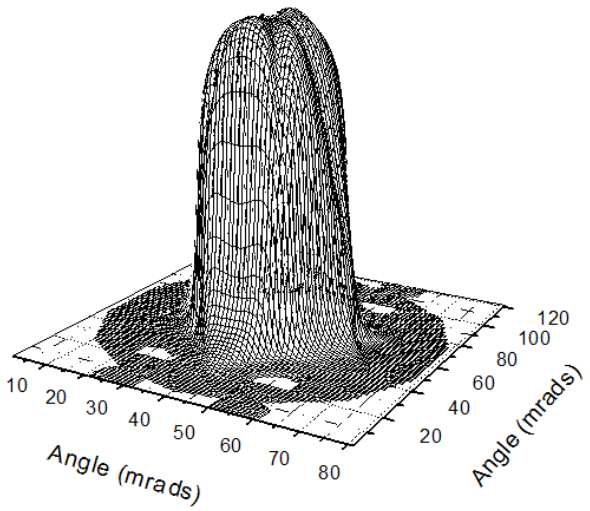

Figure 6. *Angle versus angle (eye view).*

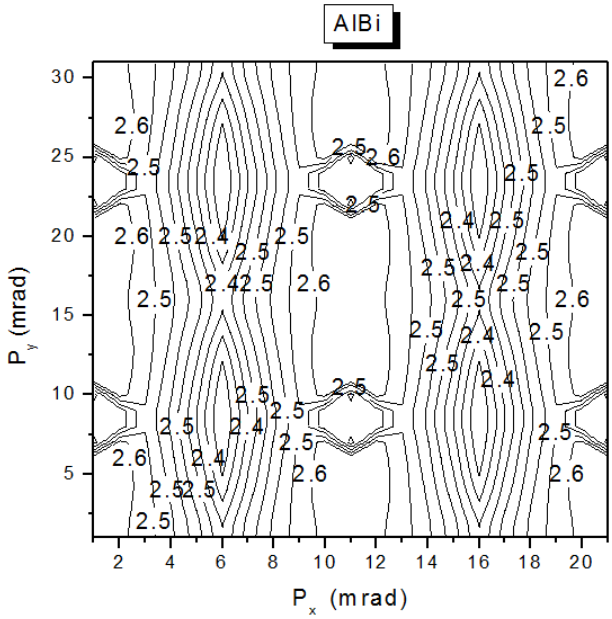

Figure 7. *Momentum along y versus momentum along x.*

Table 1. *The adjusted symmetric and antisymmetric form factors (in Ry), and the lattice constant a_o (in atomic units) for AlBi used in these calculations.*

Compound	Adjusted lattice constant a_o	Experimental lattice constant a_o [25]	Adjusted form factors	Experimental form factors [26]
AlBi	6.3354890	6.448270	$V_s(3)$=-0.31017 $V_s(8)$=0.00172 $V_s(11)$=0.0451 $V_a(3)$=0.13225 $V_a(4)$=0.09655 $V_a(11)$=0.01513	$V_s(3)$=-0.29476 $V_s(8)$=0.00385 $V_s(11)$=0.09565 $V_a(3)$=0.11583 $V_a(4)$=0.03084 $V_a(11)$=0.01265

Table 2. *The calculated Fourier coefficients of the valence charge densities for AlBi.*

$G(a/2\pi)$	Fourier coefficients (e/Ω) for AlBi
000	8.0000 0.0000
111	0.3327 -0.1258
220	0.0199 0.0736
311	-0.0199 -0.0187
222	0.0001 -0.1158
400	0.0001 0.0323
331	-0.0242 0.0075

4. Conclusion

In the present paper we have reported positronic distributions for AlBi calculated within the pseudopotential formalism and employing the independent particle model (IPM). These distributions are found to be strongly influenced by the actual symmetry of the orbitals taking part in bonding, therefore, it is expected that the positron-

annihilation technique is an effective tool and a sensitive microscopic probe of semiconductors; we have shown that by performing the electron-positron momentum densities, a deep insight into the electronic properties can be achieved. More importantly, because of its relatively few assumptions, the present theory yields a reliable single-particle description of positron annihilation. As a consequence, it represents an excellent starting point for a systematic many-particle description of the process.

References

[1] Ph. Ebert, Surf. Sci. Rep. 33, 121 (1999).

[2] B. Engels, P. Richard, K. Schroeder, S. Blügel, Ph. Ebert, and K. Urban, Phys. Rev. B 58, 7799 (1998).

[3] Dietz, R. E.; Thomas, D. G.; Hopfield, J. J. Phys. Rev. Lett. 1962, 391–393.

[4] Thomas, D. G.; Hopfield, J. J.; Frosch, C. J. Phys. Rev. Lett. 1965, 15, 857–860.

[5] Jianjian Shi, Jiaheng Wang, Wei Yang, Zhejie Zhu, Yichu Wu, Materials Research. 2016; 19(2): 316-321.

[6] E. Schroten, A. Goossens, J. Schoonman, Journal of Applied Physics Vol. 83, 1660-1663 (1998).

[7] Ric P. Shimshock Editor, "Infrared Thin Films", Deposition Sciences, Inc., Santa Rosa, CA, USA. Published 1992.

[8] M. Aki, Y. Ohno, H. Kohno and S. Takeda, Phil. Mag. A 59 (2000) 2694-2699.

[9] V. K. Gupta, C. C. Wamsley, M. W. Koch, and G. W. Wicks, J. Vac. Sci. and Technol. B 17, 1246 (1999).

[10] Yan Zhao and Donald G. Truhlar, THE JOURNAL OF CHEMICAL PHYSICS 128, 184109 (2008).

[11] J. Tao, J. P. Perdew, V. N. Staroverov, and G. E. Scuseria, Phys. Rev. Lett. 91, 146401 (2003).

[12] Y. Zhao and D. G. Truhlar, J. Chem. Phys. 125, 194101 (2006).

[13] M. Gruning, O. Gritsenko, and E. J. Baerends, J. Phys. Chem. A 108, 4459 (2004).

[14] H. Zenasni, H. Aourag, S. R. Broderick, and K. Rajan, Phys. Status Solidi B 247, No. 1, 115–121 (2010).

[15] J. Hafner et al, MRS BULLETIN • Vol. 31, (2006).

[16] Grimme, S. J. Comput. Chem., 25: 1463–1473 (2004).

[17] Jing-Jing Zheng, E. R. Margine, Phys. Rev. B 94, 064509 (2016).

[18] R. Khatri et al, AIP Conference Proceedings 1536, 419 (2013).

[19] M. Ameri, M. Fodil, Fatma Z. Aoumeur-Benkabou, Z. Mahdjoub, F. Boufadi, A. Bentouaf Materials Sciences and Applications, Vol. 3 No. 11, (2012).

[20] D. G. Green and G. F. Gribakin, Phys. Rev. A 95, 036701 (2017).

[21] X. Ma, M. Wang, Y. Zhu, Y. Liu, C. Yang, and D. Wang, Phys. Rev. A 94, 052709 (2016).

[22] K. Fujiwara, T, Hyodo, J. Phys. Soc. Jpn, 35 (1973) 1133.

[23] M. Saito, A. Oshiyama, S. Tanigawa, Private communication.

[24] W. Liu, S. Berko and A. P. Mills Jr., Positron annihilation, Matter. Sci. Forum, Szombachely, 743 (1992).

[25] R. R. Q. Freitas et al, J. Phys. Chem. C, 2015, 119 (41), pp 23599–23606.

[26] Scott Broderick, Graduate Theses and Dissertations, Iowa State University (2009).